



FULL LENGTH ARTICLE

# Targeting fructose metabolism by glucose transporter 5 regulation in human cholangiocarcinoma



Nattawan Suwannakul <sup>a</sup>, Napat Armartmuntree <sup>b</sup>,  
Raynoo Thanan <sup>b</sup>, Kaoru Midorikawa <sup>a</sup>, Tetsuo Kon <sup>c</sup>,  
Shinji Oikawa <sup>a</sup>, Hatasu Kobayashi <sup>a</sup>, Ning Ma <sup>d</sup>,  
Shosuke Kawanishi <sup>e</sup>, Mariko Murata <sup>a,\*</sup>

<sup>a</sup> Department of Environmental and Molecular Medicine, Mie University Graduate School of Medicine, Tsu, Mie 514-8507, Japan

<sup>b</sup> Department of Biochemistry, Faculty of Medicine, Khon Kaen University, Khon Kaen 40002, Thailand

<sup>c</sup> Laboratory of Functional Genomics, Graduate School of Bioscience, Nagahama Institute of Bioscience and Technology, Nagahama, Shiga 526-0829, Japan

<sup>d</sup> Graduate School of Health Science, Suzuka University of Medical Science, Suzuka, Mie 513-8670, Japan

<sup>e</sup> Faculty of Pharmaceutical Sciences, Suzuka University of Medical Science, Suzuka, Mie 513-8670, Japan

Received 21 May 2021; received in revised form 26 August 2021; accepted 11 September 2021

Available online 2 October 2021

## KEYWORDS

Cholangiocarcinoma;  
Fructose;  
Glucose transporter  
5;  
Metabolic regulation;  
Warburg effect

**Abstract** Alterations in cellular metabolism may contribute to tumor proliferation and survival. Upregulation of the facilitative glucose transporter (GLUT) plays a key role in promoting cancer. GLUT5 mediates modulation of fructose utilization, and its overexpression has been associated with poor prognosis in several cancers. However, its metabolic regulation remains poorly understood. Here, we demonstrated elevated GLUT5 expression in human cholangiocarcinoma (CCA), using RNA sequencing data from samples of human tissues and cell lines, as compared to normal liver tissues or a cholangiocyte cell line. Cells exhibiting high-expression of GLUT5 showed increased rates of cell proliferation and ATP production, particularly in a fructose-supplemented medium. In contrast, GLUT5 silencing attenuated cell proliferation, ATP production, cell migration/invasion, and improved epithelial–mesenchymal transition (EMT) balance. Correspondingly, fructose consumption increased tumor growth in a nude mouse xenograft model, and GLUT5 silencing suppressed growth, supporting the tumor-inhibitory effect of GLUT5 downregulation. Furthermore, in the metabolic pathways

\* Corresponding author. Fax: +81 59 231 5011.

E-mail address: [mmurata@med.mie-u.ac.jp](mailto:mmurata@med.mie-u.ac.jp) (M. Murata).

Peer review under responsibility of Chongqing Medical University.

of fructolysis-Warburg effect, the expression levels of relative downstream genes, including ketohexokinase (KHK), aldolase B (ALDOB), lactate dehydrogenase A (LDHA), and monocarboxylate transporter 4 (MCT4), as well as hypoxia-inducible factor 1 alpha (HIF1A), were altered in a GLUT5 expression-dependent manner. Taken together, these findings indicate that GLUT5 could be a potential target for CCA therapeutic approach via metabolic regulation.

Copyright © 2021, Chongqing Medical University. Production and hosting by Elsevier B.V. This is an open access article under the CC BY-NC-ND license (<http://creativecommons.org/licenses/by-nc-nd/4.0/>).

## Introduction

Cellular metabolism is a fundamental biological process that consumes or produces energy and macromolecules required for cell growth and homeostasis. Alteration in cellular metabolism is a hallmark of carcinogenesis, implicating uncontrolled proliferation.<sup>1</sup> In contrast to normal cells, where the cellular fuel is mainly produced via mitochondrial oxidative phosphorylation, cancer cells predominantly rely on cytosolic glycolysis, even under the aerobic conditions.<sup>2</sup> The phenomenon of aerobic glycolysis, or the Warburg effect, in cancer cells tends to convert glucose to lactate, which is a source of energy and is involved in tumor progression.<sup>3</sup> Since the Warburg effect produces less ATP, an increase in glucose uptake is necessary to elevate energy supply for tumor growth.<sup>4</sup>

Following glucose, fructose is the second most common dietary carbohydrate and is abundant in modern diets. Fructose is metabolized and integrated with glucose degradation to produce cellular energy, suggesting that fructose, like glucose, may provide energy for cell growth.<sup>5</sup> High fructose consumption is correlated with the development and aggressiveness of metabolic diseases and cancers.<sup>6,7</sup> In contrast to glucose, fructose metabolism produces higher levels of ATP and fatty acids in lung cancer cells.<sup>8</sup> Moreover, in pancreatic cancer, fructose is preferentially utilized for nucleic acid synthesis, promoting its cancer proliferative capacity, which is greater than glucose.<sup>9</sup>

Glucose is transported between the intracellular and extracellular compartments by glucose transporters (GLUTs). The 14 GLUT subtypes found in humans exhibits distinct affinities for sugars, such as glucose, fructose, galactose, and mannose and a tissue-dependent expression.<sup>10</sup> GLUT5, encoded by the *SLC2A5* gene, is a high-affinity transporter for fructose, which is mainly located at the apical surface of intestinal epithelial cells.<sup>11</sup> In breast cancer cells, the expression of GLUT5 is associated with the rate of fructose uptake and is related to tumor progression and metastasis.<sup>12</sup> Moreover, upregulation of GLUT5 was found to be highly correlated with a poor prognosis in patients with lung cancer.<sup>13</sup> Thus, the regulation of GLUT5 expression might be a potential target for cancer therapy. In this study, we focused on cholangiocarcinoma (CCA), which is a clinically silent cancer with poor overall survival and prognosis. In order to clarify the roles of GLUT5 and fructose metabolism in the development of CCA, we assessed GLUT5 expression levels in CCA tissues and in CCA cell lines compared with their normal

counterparts. To determine whether GLUT5 facilitates cell proliferation in CCA, cell viability response to a GLUT5 inhibitor and depletion of GLUT5 using GLUT-siRNA was assessed in the presence of fructose supplementation. The tumor-suppressing effects of GLUT5 silencing were further assessed using human CCA cell lines, accompanied by fructose uptake and ATP production. In addition, we performed nude mouse xenografts of GLUT5-silencing CCA cells to evaluate whether fructose might enhance tumor growth in CCA and the effect of GLUT5 knockdown. To investigate the mechanism underlying GLUT5-mediated cells proliferation in CCA, we examined the levels of gene expression in fructose metabolic pathway.

## Materials and methods

### Human tissue samples

The expression of GLUT5 in CCA was determined using immunohistochemical staining of human tissue samples and the clinicopathological characteristics of the tumors were compared. Fifty human tissue samples were obtained from the Cholangiocarcinoma Research Institute of Srinagarind Hospital, Khon Kaen University, Thailand. All human tissues samples were collected with the approval of the Ethics Committee for Human Research (HE571283), Khon Kaen University, Thailand, after obtaining informed consent from the patients. In addition, three independent tissue microarrays, including two intrahepatic CCA tissue samples (LV1004;  $n = 100$  and HIBD-Ade100PG-01;  $n = 100$ ) with adjacent normal liver tissue samples (LV801;  $n = 21$ ) were purchased from US Biomax (Derwood, Maryland, USA). Clinical characteristics is described in [Table S1](#).

### Histological and immunohistochemical (IHC) studies

Tumor tissue samples from humans and mice were fixed overnight in 4% paraformaldehyde, followed by dehydration and paraffin infiltration. The embedding and sectioning procedures were then performed to construct 5  $\mu\text{m}$  sections using Leica Microsystems (Wetzlar, Germany). Histological changes were observed by hematoxylin and eosin (H&E) staining under a light microscope (Olympus, Tokyo, Japan). The expression levels of GLUT5 and Ki67 were determined by IHC staining. Tumor sections were subjected to dewaxing, rehydration, and antigen retrieval, as previously described.<sup>14</sup> After blocking endogenous peroxidase activity by incubation in 1% skim milk for 25 min at room

temperature, sections were incubated overnight with a primary antibody in a humid chamber. Following three washes, the sections were subsequently treated with a specific biotinylated secondary antibody and avidin-biotin-peroxidase conjugate (Vector Laboratories, Burlingame, CA, USA). Immunoreaction was visualized by incubation with a DAB peroxidase substrate kit (Nacalai Tesque, Kyoto, Japan) and counterstained with hematoxylin. The expression level of GLUT5 was evaluated using a light microscope (Olympus). Based on overall intensity, a scoring system for IHC staining was used as follows: scores of 0 (no staining), 1 (weak staining), 2 (moderate staining), 3 (strong staining) and 4 (very strong staining) were assigned to normal bile duct cells and CCA tissues. Antibody information is described in Table S2.

### Cell culture, modulation of sugar concentration in culture medium, and GLUT5 inhibitor treatment

Human cell lines comprising the cholangiocyte cell line (MMNK-1 [RRID:CVCL\_M266]) and two cholangiocarcinoma cell lines (KKU-213A [RRID:CVCL\_M261] and YSCCC [RRID:CVCL\_3629]) were used in this study. MMNK-1 and KKU-213A were purchased from the Japanese Collection of Research Bioresources Cell Bank (Osaka, Japan), and YSCCC was purchased from the RIKEN Bioresource Research Center (Ibaraki, Japan). MMNK-1 and KKU-213A cells were maintained in DMEM medium (#11885–084, Gibco, Thermo Fisher Scientific, Waltham, MA, USA) supplemented with 5% and 10% (v/v) fetal bovine serum (FBS; CELLect, MP Bio-medicals, CA, USA), respectively. The YSCCC cells were cultured in RPMI-1640 medium (#11875–093, Gibco, Thermo Fisher Scientific) supplemented with 10% FBS. All cell lines were grown at 37°C in a humidified incubator with 5% CO<sub>2</sub>. All human cell lines have been authenticated using short tandem repeat profiling within the last three years. All experiments were performed with mycoplasma-free cells.

In a few experiments, glucose-free DMEM (#11966–025), glucose-free RPMI (#11879–020), and dialyzed FBS (#A3382001) were used (Gibco, Thermo Fisher Scientific) to assess the effects of fructose. D-Fructose was purchased from Sigma–Aldrich (St. Louis, MO, USA). Based on the standard culture medium containing 5.6 mM glucose for CCA culture, we modulated the concentration of sugar (either fructose or glucose) to 0, 0.7, 1.4, 2.8, or 5.6 mM, using glucose-free medium for a few experiments. These fructose- or glucose-modulated media were supplemented with 10% dialyzed FBS. To inhibit GLUT5 expression, cells were pretreated with 2,5-anhydro-D-mannitol (2,5-AM; Funakoshi, Tokyo, Japan) at various concentrations (0, 0.25, 0.5, 1, and 2 mM) for 72 h.

### RNA sequencing

To monitor the gene expression profile, we initially carried out RNA sequencing on two different cell lines, MMNK-1 ( $n = 3$ ) and KKU-213A ( $n = 2$ ) and compared them. Total RNA was extracted using the NucleoSpin RNA Plus kit (Takara, Shiga, Japan) following the manufacturer's protocol and the purity was quantified using a NanoDrop

spectrophotometer and agarose gel electrophoresis. RNA sequencing was performed on an Illumina NovaSeq 6000 (Takara). After alignment, fragments per kilobase of exon per million mapped fragments (FPKM) values were used to measure the differentially expressed genes in samples. The relative fold change of gene expression was presented as the alteration of log<sub>2</sub> FPKM of the sample with normalized control. The sequencing coverage and quality statistics for each sample are summarized in Table S3. Additionally, expression data from The Cancer Genome Atlas (TCGA) in CCA were obtained from the University of California Santa Cruz Xena (<https://xenabrowser.net/datapages>), containing nine normal bile duct tissue samples and 36 CCA tissue samples. The gene expression profile was generated using the Illumina HiSeq 2000 RNA Sequencing platform, and data were obtained on the gene-level transcription estimates as in log<sub>2</sub>(x+1) transformed RSEM normalized count.

### Cell viability

Cell viability was evaluated by the MTT assay. Briefly, 10 μL of 5 mg/mL MTT solution (Merck, Burlington, MA, USA) was added to each well and incubated for 4 h at 37°C. The formazan crystals were then dissolved in 150 μL DMSO (Wako, Osaka, Japan) and cell viability was quantified at an absorbance of 570 nm using a microplate reader (Bio-Rad, Hercules, CA, USA).

### RNA interference

CCA cells were transiently transfected with small interfering RNA (siRNA) using Lipofetamine 3000 (Invitrogen, Thermo Fisher Scientific) in an antibiotic-free culture medium. Negative siRNA (SIC-001-10) and siRNA targeting SLC2A5 were purchased from Sigma–Aldrich with two different sequences: siRNA#1 (SASI\_Hs01\_00157409) and siRNA#2 (SASI\_Hs01\_00157411). For transfection in 6-well plates, CCA cells ( $0.2 \times 10^6$  cells/well) were treated with negative control or targeting siRNA at a final concentration of 40 nM following the manufacturer's recommendations in a CO<sub>2</sub> incubator at 37°C for 48 h. The cell culture medium was then replaced with a complete culture medium, and the transfected cells were harvested for further experiments.

### RNA isolation and quantitative real-time polymerase chain reaction (RT-qPCR)

The gene expression levels and efficiency of siRNA transfection were determined using RT-qPCR at 48 h post-transfection. Total RNA was extracted using TRIzol reagent (Thermo Fisher Scientific), and the quality of RNA was determined by measuring the 260/280 ratio, as previously described.<sup>14</sup> cDNA was synthesized using the High-Capacity RNA-to-cDNA Kit (Applied Biosystems, Thermo Fisher Scientific). Twenty nanograms of cDNA was used as the template in qPCR using Applied Biosystems StepOne™ and StepOnePlus™ Real-Time PCR Systems (Applied Biosystems). Primers were obtained from Applied Biosystems TaqMan Gene Expression Assays (Waltham, MA, USA), which included SLC2A5 (Assay ID Hs01086390\_m1) and GAPDH

(Assay ID Hs99999905\_m1) as an internal control. Thermal cycling was carried out at 95°C for 10 min, followed by 50 two-step cycles, as follows: 95°C for 15 s and 60°C for 1 min. The relative fold change of expression levels was normalized to GAPDH and calculated using the  $2^{-\Delta\Delta CT}$  method.

### ATP measurement

To quantify the amount of ATP produced following different sugar treatments, the level of ATP was determined using an ATP assay kit (Ab83355, Abcam, Cambridge, MA, USA) according to the manufacturer's instructions. We resuspended  $1 \times 10^6$  cells in an assay buffer and deproteinized the sample using the HClO<sub>4</sub>/KOH method. After separation by centrifugation, the supernatant was mixed with the reaction mixture in a 96-well plate and incubated at room temperature for 30 min, in the dark. ATP levels were determined at an absorbance of 570 nm in three independent experiments and calculated using the equation provided by the manufacturer's instruction.

### Fructose uptake assay

Under the different conditions of presence and absence of fructose supplementation, the ability of cellular fructose uptake was evaluated in CCA cells, following the manufacturer's instruction (MAK265, Sigma–Aldrich). In 6-well plates, siRNA-transfected cells were seeded in sugar-free medium for 24 h and then pre-incubated with a medium supplemented with or without 5.6 mM fructose for at 37°C for 72 h. Each group of  $1 \times 10^6$  cells were homogenized in 100  $\mu$ L assay buffer and centrifuged. In duplicate, 50  $\mu$ L supernatant was mixed with 50  $\mu$ L of the reaction mixture and incubated in the dark at 37°C for 2 h. The amount of fructose level was measured at an absorbance of 570 nm in three independent experiments and calculated using the equation provided by the manufacturer's instruction.

### Cell migration and invasion

The effect of GLUT5 downregulation on cell mobility was assessed using a Transwell migration/invasion assay. Following siRNA transfection, in the invasion experiment, cell solution ( $1 \times 10^5$  cells) in 500  $\mu$ L serum-free medium containing glucose or fructose (5.6 mM) was added to the Matrigel-coated insert of 24-well Transwell plate, 8  $\mu$ m pore size (Corning Incorporated, Corning, NY, USA), and filled the lower chamber was filled with 750  $\mu$ L FBS-containing medium. After incubation at 37°C for 24 h, the non-invaded cells were removed by gentle swabbing, and the membranes were fixed and stained with a cell stain solution (Cell Biolabs, San Diego, CA, USA) for 10 min at room temperature and allowed to air dry. In the migration experiment, cells were added to the control insert without Matrigel coating, and the subsequent steps were carried out similar to the invasion experiment. The number of invaded or migratory cells was counted under a microscope in five random fields. Each assay was performed in triplicate.

### Wound healing assay

The motility of CCA cells following siRNA was monitored using a wound healing assay. In brief, cells were seeded at  $1 \times 10^5$  cells per well in 6-well plates and incubated with siRNA in triplicate. After the cells reached 90%–95% confluence, each well was scratched using a 200  $\mu$ L pipette tip and gently washed with a serum-free medium. The cells were maintained in a culture medium containing glucose or fructose. Wound closure was monitored microscopically at 0, 10, 22, and 30 h. The wound distance was quantified by measuring the average width of the wounds using ImageJ software (National Institutes of Health, Bethesda, MA, USA) and the percentage of wound distance was calculated by comparing the area at 0 h in each group.

### Western blot

Protein expression levels were quantified using Western blot analysis. Treated cells were lysed by treatment with RIPA buffer containing 1 mM phenylmethylsulfonyl fluoride (PMSF) on ice for 5 min. After cold centrifugation, the supernatant was separated, and the protein concentration of the samples was determined using the Coomassie Protein Assay Kit (Thermo Fisher Scientific) at 595 nm. Equal amounts of protein (20–30  $\mu$ g) were then subjected to electrophoresis on a 5%–20% polyacrylamide gradient gel (Wako) and transferred to a 0.2  $\mu$ M polyvinylidene difluoride (PVDF) membrane (Merck). Blocking step was subsequently performed in 5% skim milk at room temperature for 30 min. Membranes were probed with primary antibodies (Table S2) at 4°C, overnight. Following triple washing with Tris-buffered saline-Tween20, the membranes were incubated with horseradish peroxidase-conjugated secondary antibodies (Table S2) at room temperature for 1 h. The immunoreactive bands were developed using the enhanced chemiluminescence detection kit reagents (GE Healthcare, CA, USA) and detected using LAS4000mini (Fujifilm, Tokyo, Japan). ImageJ software was used for quantitative analysis of relative protein expression of targets and GAPDH or  $\beta$ -actin. All targets were evaluated in triplicate.

### In vivo tumorigenicity

Experiments were performed on male athymic BALB/c nude mice (4 weeks of age) purchased from Japan SLC Inc. (Hamamatsu, Japan). All experimental procedures were conducted according to the protocol approved by the Committee of Animal Center of Mie University, Mie, Japan (Approval no. 26-19-sai3). All mice were maintained under the specific pathogen-free conditions in a 12-12 h dark/light cycle with free access to food and water *ad libitum*. After a week of acclimatization, the mice were divided into three groups ( $n = 8$  mice per group) for treatment with different types of siRNA-transfected cells and were allowed to drink a fructose solution. The mice were individually subcutaneously injected with KKU-213A cells ( $2 \times 10^6$  cells/100  $\mu$ L PBS) at the right flank with negative control siRNA (groups 1 and 2) and GLUT5 siRNA#2 (group 3). After tumor inoculation, the mice were allowed to freely drink distilled water (DW) (group 1) and 15% fructose solution (groups 2

and 3). Their body weight and tumor volume were monitored every two days, and fluid consumption was recorded every three days. Following four weeks of treatment, all the mice were then sacrificed. Solid tumors were separated for immunohistochemical staining.

### Statistical analysis

Student's *t*-test was used to assess the differences in gene expression levels and functional alterations between the groups. The nonparametric Kruskal–Wallis test or Mann–Whitney test was used to analyze the differences between IHC scores and clinical characteristics in human tissue samples. All statistical analyses were performed using the Statistical Program for Social Sciences (SPSS 23.0; IBM Corp., Armonk, NY, USA). Statistical significance was set at  $P < 0.05$ .

## Results

### GLUT5 expression is upregulated in human CCA cell lines and tissues

We initially assessed the differential gene expression in normal cholangiocytes (MMNK-1) and CCA (KKU-213A) cells using RNA-Seq analysis, and found diversity in the expression levels of the SLC2A family, in terms of the down-regulation of SLC2A2, SLC2A6, SLC2A8, SLC2A11, and SLC2A14. However, upregulation of SLC2A1, SLC2A5, SLC2A9, and SLC2A13 was observed, whereas there was no difference observed in SLC2A3 and SLC2A7 expressions (Fig. 1A bar chart), particularly SLC2A5 overexpression was presented in CCA samples (Fig. 1A heatmap). According to the data regarding the upregulated levels of SLC2A family in CCA cells, protein expression levels by Western blot showed the upregulations of SLC2A/GLUTs family in CCA cells, including GLUT1, GLUT5, GLUT9, and GLUT13, remarkably the overexpression of GLUT5 was found in both CCA cell lines (Fig. 1B). Thus, we focused on GLUT5, which might be a key protein target relevant to CCA.

The gene expression of SLC2A5/GLUT5 in CCA cell lines KKU-213A and YSCCC, along with a normal cell line MMNK-1, were determined using RT-qPCR and demonstrated significantly higher expression levels of SLC2A5 in both CCA cell lines compared to normal cells (Fig. 1C). We subsequently verified this finding using the public TCGA database ( $n = 45$ ), and the expression of SLC2A5 was found to be significantly higher in CCA tissue samples than in normal tissues (Fig. 1D). Moreover, to validate the expression profile from the TCGA database, the qualitative and quantitative levels of GLUT5 protein were determined by IHC staining of tissue microarrays and our samples. Overexpression of GLUT5 was clearly detected in CCA tissue samples with high IHC scores compared to normal bile duct cells in liver tissues (Fig. 1E). Interestingly, the expression levels of GLUT5 were significantly elevated in the higher pathologic T (3–4) groups and stages III–IV than in the lower pathologic T (0–2) groups and stages I–II, respectively (Fig. 1F). Collectively, these results suggest that a high expression of SLC2A5/GLUT5 may be involved in CCA progression.

### Fructose enhances CCA cell proliferation

The MTT assay was performed to explore the effect of glucose and fructose on cell proliferation in normal and CCA cells. As shown in Figure 2A, in the glucose-containing medium, steady growth rates were observed in both normal and CCA cell lines in a dose-dependent manner, except for a slight decline seen in YSCCC cells at 5.6 mM glucose. In fructose-supplemented medium, although the normal MMNK-1 cells could not grow, CCA cells grew in a concentration-dependent manner.

We examined the effect of inhibition of fructose transportation on cell proliferation using various concentrations of 2,5-AM. In normal cells, 2,5-AM showed no effect on cell proliferation in either glucose- or fructose-supplemented medium (Fig. 2B, top). In contrast, CCA cell lines showed a dose-dependent suppression, which was more pronounced in the fructose-supplemented medium (Fig. 2B, middle and bottom). Collectively, these data support the hypothesis of a growth-promoting effect of fructose in CCA cells, but not in normal cells.

### CCA cells exhibit high levels of fructose uptake and ATP production

To further determine the variation in fructose consumption in CCA cells, the amount of cellular fructose was evaluated after incubating in a medium supplemented with or without fructose. In the fructose-supplemented medium, compared with normal cells, KKU-213A and YSCCC cells had significantly higher fructose levels, predominantly KKU-213A cells (Fig. 2C).

In addition, the amount of cellular ATP was measured to investigate the potential of ATP production in distinct cell types and sources of sugar utilized, including glucose and fructose. In CCA cell lines, ATP production was significantly higher in fructose-supplemented medium than in glucose-supplemented medium, but the inverse relationship was seen in normal cells. ATP production in CCA cells was significantly higher than that in normal cells in the presence of fructose supplementation. Interestingly, amongst fructose-supplemented medium, GLUT5 inhibition with 2,5-AM (2 mM) showed a significant reduction of ATP level in CCA cells, but did not affect in normal cells (Fig. 2D). All the above findings imply that GLUT5 may facilitate fructose uptake in CCA cells and that fructose might be a more potent source of ATP production than glucose.

### GLUT5 silencing inhibits CCA cell growth and fructose utilization

To elucidate the biological function of GLUT5 in CCA development, siRNA was used to transiently knockdown GLUT5 in CCA cell lines, and the cell proliferative effect was then measured using an MTT assay. The mRNA and protein levels of GLUT5 are shown in Figure 3A and B. The expression of GLUT5 was significantly decreased in KKU-213A and YSCCC cells. Compared to the control, cell proliferation was considerably suppressed in GLUT5 knockdown cells in a time-dependent manner, particularly a fructose-supplemented medium (Fig. 3C, D). Cellular

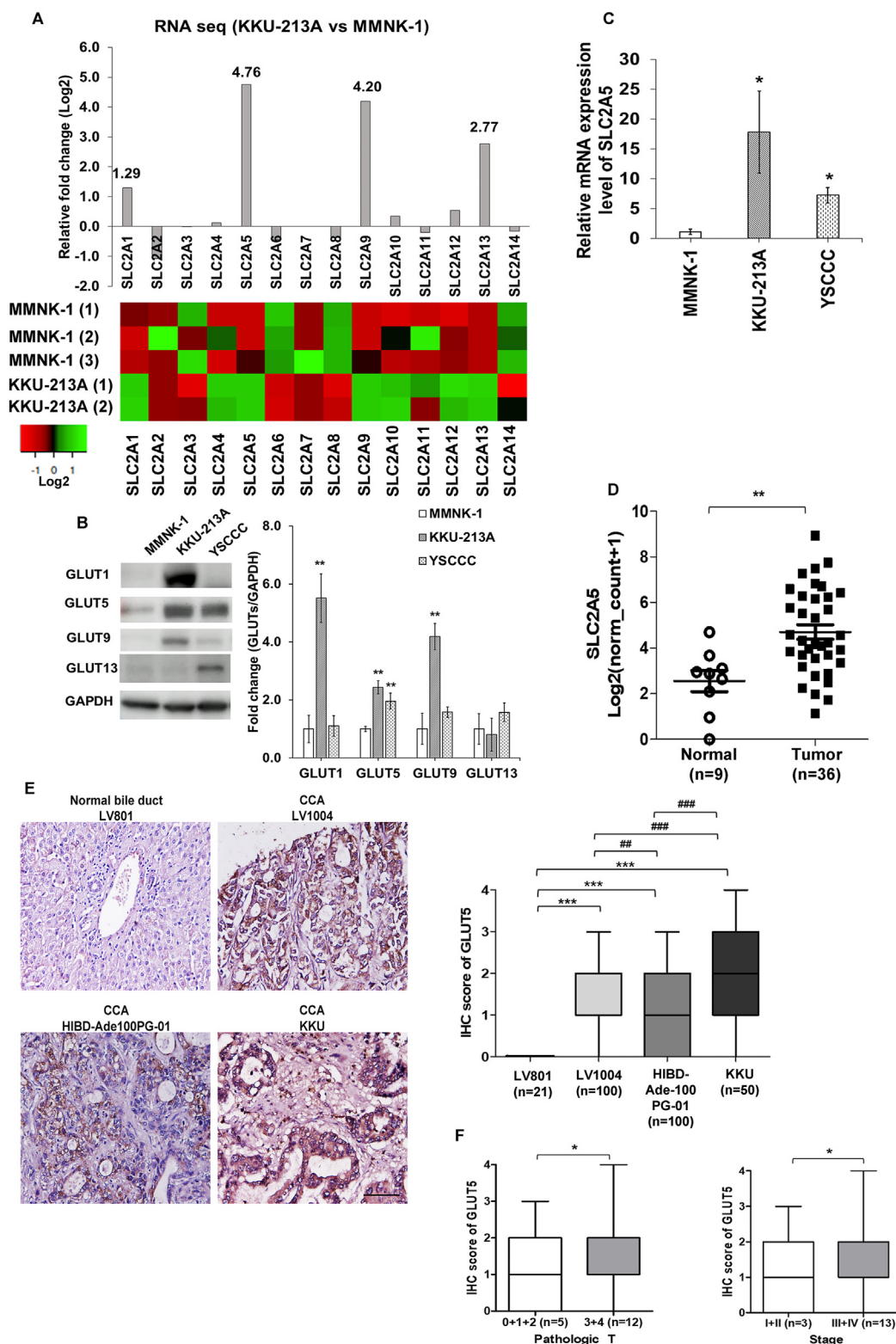


**Figure 1** Overexpression of GLUT5 in human CCA tissue samples. **(A)** Gene expression levels of SLC2A family including SLC2A5 in MMNK-1 and KKU-213A cells using RNA sequencing (bar chart and heatmap). **(B)** Protein levels of GLUT family (GLUT1, GLUT5, GLUT9 and GLUT13) and **(C)** SLC2A5 mRNA in normal and CCA cell lines. **(D)** SLC2A5 RNA levels in TCGA database. **(E)** IHC scores of GLUT5 in human tissue microarray and patient samples. **(F)** IHC staining score of tumor tissues compared between pathologic T 0 + 1+2 vs. 3 + 4 (left) and stage I + II vs. III + IV (right). \* Significant difference compared to normal bile duct cells (MMNK-1) or normal bile duct cells in liver tissues (LV801). # Significant difference between CCA tissues. One mark (\*, #) indicates  $P < 0.05$ , two marks indicate  $P < 0.01$ , three marks indicate  $P < 0.001$ .

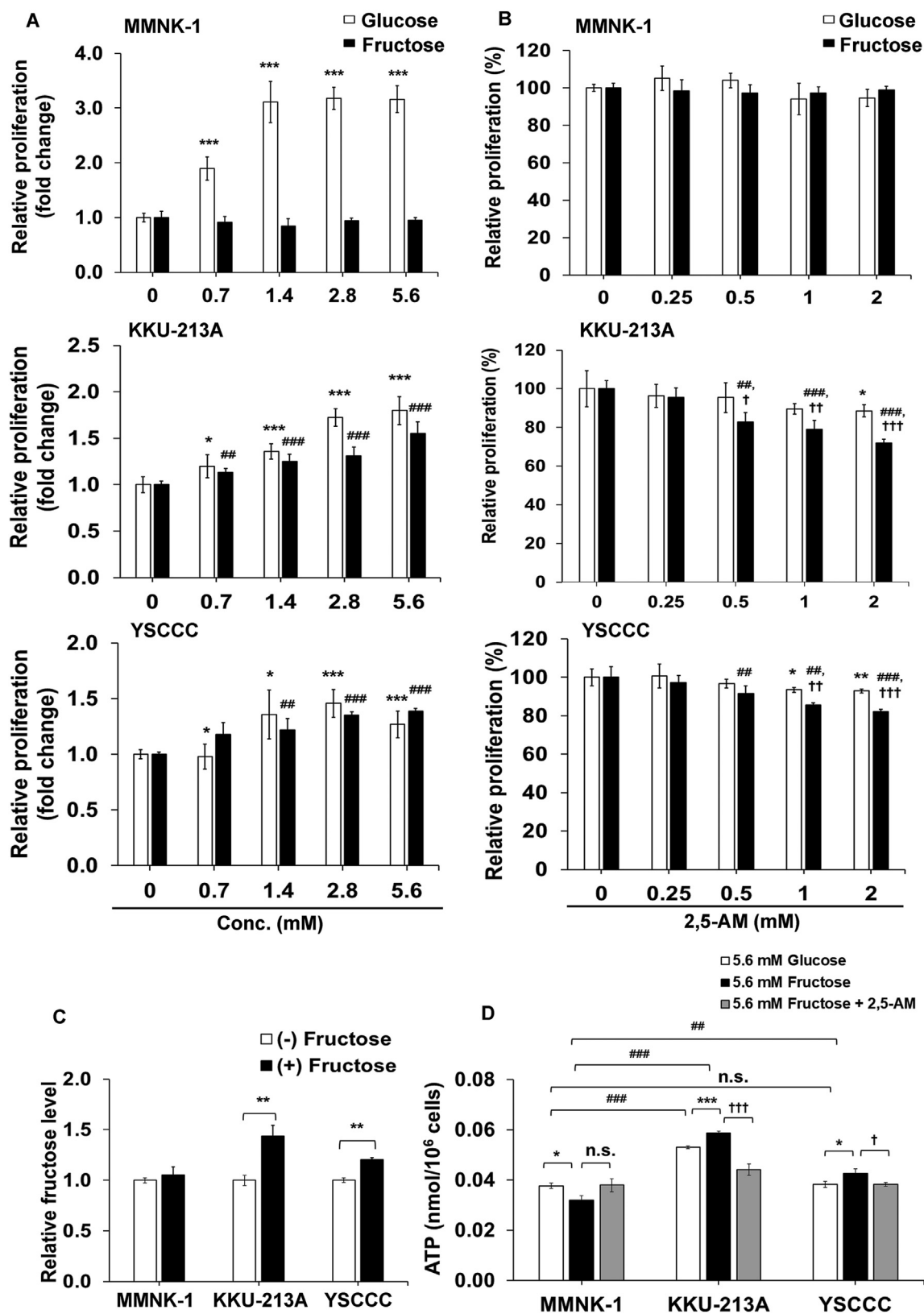


**Figure 2** Effect of fructose on cell growth, intracellular fructose levels and ATP production. **(A)** Cell proliferation of CCA cells in glucose- or fructose-supplemented medium. Marks indicate significant difference compared to the zero concentration (no sugar condition, as 1) of glucose-supplemented medium (\*) or fructose-supplemented medium (†). **(B)** Inhibitory effect of cell proliferation in CCA cells (5.6 mM glucose/fructose) treated with 2,5-AM at various concentrations of 0, 0.25, 0.5, 1, and 2 mM for 72 h. Relative proliferation (%) was adjusted the cell proliferation in CCA cells treated with 2,5-AM at 0 mM (100% proliferation). \* †

fructose uptake was consistently reduced in GLUT5 knockdown cells in the fructose-supplemented medium, but there was no alteration in fructose uptake in the fructose-free medium (Fig. 3E, F). These results indicated that downregulation of GLUT5 may control CCA proliferation and fructose uptake.

### GLUT5 silencing suppresses cell invasion/migration and EMT in CCA cells

Matrigel and Transwell chamber assays were used to investigate the role of GLUT5 in cell invasion and migration in CCA cells. GLUT5 knockdown cells, KKKU-213A and YSCCC, showed a significant reduction in the number of invaded (Fig. 4A) and migratory (Fig. 4B) cells when compared to control cells. By the differential energy source, despite those suppressive abilities were shown in CCA cells cultured in both glucose- and fructose-supplemented medium, cells in fructose-containing medium was found to be more effective at inhibiting cell invasion and migration than that in glucose-containing medium. Similarly, additional validation of cell migration was obtained using a wound healing assay. Wound closure was suppressed, demonstrated by longer distances in GLUT5 knockdown cells, compared with the control cells, which was potentially affected in fructose-supplemented medium (Fig. 4C).

Furthermore, metastatic potential of the cells was analyzed via EMT to determine whether GLUT5 expression affects cell invasion/migration in CCA cells. The results revealed that the protein expression level of the epithelial-like cell marker, E-cadherin, was upregulated and the protein expression level of the mesenchymal-like cell marker, N-cadherin, was downregulated in GLUT5 knockdown cells either by GLUT5 inhibitor (2 mM of 2,5-AM, Fig. 4D) or gene knockdown (siRNA, Fig. 4E), compared to control cells. Collectively, the inhibition of GLUT5 expression might suppress invasion and migration of CCA cells by inhibiting EMT.

### GLUT5 silencing attenuates CCA tumor growth in nude mouse xenografts

We further studied GLUT5-mediated regulation of tumor growth in a mouse model. Among fructose-drinking mice, higher body weight (days 16–28) was observed compared to water-drinking mice (Fig. 5A). Fructose consumption significantly enhanced the tumor growth with higher tumor volume and weight in comparison between the two siControl groups. GLUT5 silencing remarkably reduced tumor volume and weight compared with the siControl group, in which the mice consumed fructose (Fig. 5B–D). By IHC staining showed that the expression level of GLUT5 was significantly diminished in the knockdown group, but no

alteration was observed in the control group treated with water or fructose (Fig. 5E). Moreover, tumors from both of two siControl groups exhibited an increased nuclear expression of Ki67 and its expression level was suppressed in GLUT5 knockdown group, which indicated that the GLUT5 silencing could inhibit *in vivo* tumor growth.

### GLUT5 regulates fructose metabolism in CCA development in relation to the Warburg effect

To clarify the underlying downstream pathway of GLUT5 regulation in human CCA, the protein expression of genes involved in fructose metabolism was assessed by Western blot. CCA cells showed the relatively higher levels of the genes involved in fructose metabolism, including ketohexokinase (KHK) and aldolase B (ALDOB), compared with normal MMNK-1 cells (Fig. 6A). Moreover, CCA cells expressed an elevated level of genes associated with the Warburg effect in CCA such as, lactate dehydrogenase A (LDHA), along with enhanced expression level of monocarboxylate transporter 4 (MCT4) or lactate transporter to support glycolytic activity in the cancer cells. Interestingly, hypoxia-inducible factor 1 alpha (HIF-1 $\alpha$ ) was upregulated in CCA cells (Fig. 6A). In order to verify GLUT5 mediated regulation of metabolic signaling in CCA, we performed Western blot analyses and confirmed that the expression of these target genes was inhibited in GLUT5 knockdown cells (Fig. 6B), suggesting that GLUT5 might play a role in metabolic control promoting CCA progression.

## Discussion

Fructose is a fundamental fuel for cancer cells and exerts tumor-promoting effects on cancer progression.<sup>15</sup> Despite the presence of recent research on the role of GLUT5 in tumorigenesis, the evident relationship remains to be explored. Although glucose and fructose are able to contribute to similar effects in terms of cell survival and proliferation,<sup>12</sup> they are driven by different metabolic signaling pathways. Interestingly, fructose appears to be more easily metabolized than glucose because fructose can bypass the rate-limiting step in glycolysis, and its metabolism is insulin-independent.<sup>16</sup> This suggests that fructose could be considered as an important energy source in glucose-deficient conditions, especially in the scenario of increased demand of energy from cancer cells, such as in pancreatic, breast, and liver cancers.<sup>9,17,18</sup> In present study, we demonstrated that cellular uptake of fructose was elevated in CCA cells to stimulate cancer cell growth and ATP production, but not in normal cholangiocyte cells. Our findings support the hypothesis that fructose is able to enhance the proliferation of CCA cells and is more potent, compared to glucose.

Significant difference compared to the zero concentration. † Significant difference compared between glucose- and fructose-supplemented media at the same concentration. (C) Cellular fructose uptake in CCA cell lines. \* Significant difference compared to (–) Fructose group. (D) Quantitative ATP production in CCA cell lines in differential sugar source and GLUT5 inhibitor treatment. \* Significant difference compared to glucose-supplemented medium. † Significant difference compared to normal bile duct cells (MMNK-1). † Significant difference compared to fructose-supplemented medium. One mark (\*, †) indicates  $P < 0.05$ , two marks indicate  $P < 0.01$ , three marks indicate  $P < 0.001$ . n.s., not significant.

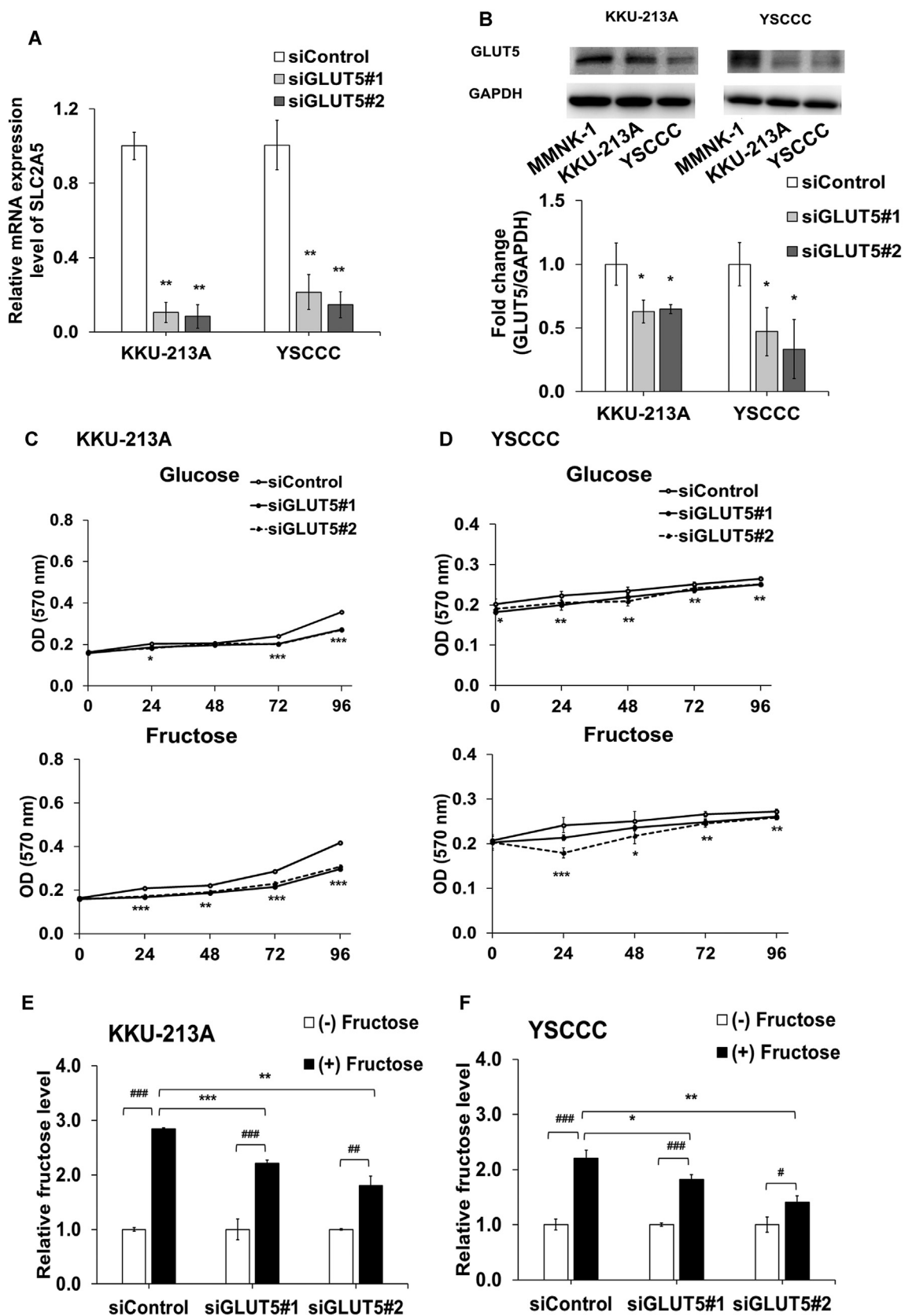


**Figure 3** Effect of GLUT5 knockdown on cell growth and intracellular fructose levels. (A) mRNA and (B) protein expression levels of GLUT5 in GLUT5 knockdown CCA cell lines. \* Significant difference compared to siControl group in each cell line. Cell viability of GLUT5 knockdown cells including (C) KKU-213A and (D) YSCCC cells in glucose- or fructose-supplemented medium. X-axis (incubation time, h) \* Significant difference compared to the siControl group in each condition. Cellular fructose uptake in GLUT5

GLUT5, a sole transporter specific for fructose, plays a crucial role in allowing the transcellular uptake of fructose normally from the lumen of the intestine into the enterocyte by facilitated diffusion,<sup>19</sup> and its overexpression has been observed in various types of cancer, such as lung, renal, ovarian, and myeloma.<sup>20–23</sup> Correspondingly, in this study, we showed the upregulation of SLC2A5 in human CCA tissue samples using the TCGA database. Our IHC analyses indicated the upregulation of GLUT5 in CCA tissues and higher IHC scores of GLUT5 in higher pathologic T and stage groups. High expression levels of GLUT5 in human CCA cell lines promote cell proliferation. Together, our results endorse the proliferative inhibition when using a GLUT5 inhibitor (2,5-AM). Simultaneously, GLUT5 was found to be involved in carcinogenic processes by regulating cell motility, migration/invasion, and transformation which was evident through GLUT5 silencing. These data indicated that GLUT5 could efficiently act as a tumor-promoting mediator during CCA proliferation and progression. Collectively, our findings verified the overexpression of GLUT5 in CCA tissue samples using web-based tools, human tissues, and human cell lines. GLUT5 upregulation was related to fructose-mediated *in vitro* cell proliferation, ATP production, migration/invasion, and *in vivo* tumor growth. In addition, our study illustrated the significant function of GLUT5 in regulating the metabolic pathway of fructose involved in CCA development. Regarding to the results of the metabolic alterations between glucose- and fructose-supplemented medium, the presence of fructose could be potentially attributed to CCA progression by ability of tumor-promoting effect and prone to fructose utilization for higher ATP production, compared to glucose condition. Simultaneously, GLUT5 knockdown suppressed tumor cell proliferation and migration/invasion at some extents, also in glucose-containing condition, although GLUT5 is a specific fructose transporter with a low affinity for glucose.<sup>24,25</sup> The phenomena were consistent with the report that cell viability of colon cancer HT-29 cells were decreased by the treatment of a GLUT5 inhibitor either in the presence or absence of fructose.<sup>26</sup> In most cancer cells, GLUT5 overexpressing cells exhibited a magnifying rate of fructose uptake, suggesting that fructose was perhaps the preferred energetic substrate supporting cell growth and proliferation. In addition to an energy expenditure, GLUT5 has been associated with cancer cell migration induced by metabolic changes.<sup>27</sup> However, the underlying metabolic changes regulated by knockdown of GLUT5 in surviving or metastatic cancer cells still need to be determined.

The metabolism of dietary fructose is primarily in the liver, and occasionally in the small intestine, where the primary site of GLUT5 expression depends on the amount of fructose consumption. Upon entering hepatocytes or enterocytes, fructose is rapidly metabolized to fructose-1-phosphate (F-1-P) by ketohexokinase (KHK) and subsequently cleaved into dihydroxyacetone phosphate (DHAP) and glyceraldehyde (GA) by aldolase B (ALDOB), prior to glycolytic ATP production.<sup>28</sup> However, ATP generated by a

primitive aerobic glycolysis is insufficient for the vast energy demand in cancer cells. Therefore, the production of lactate from glycolysis is required for cancer proliferation, even in an aerobic environment, and is called the “Warburg effect”.<sup>29</sup> Compared to glycolysis in normal cells, pyruvate is largely converted to lactate by lactate dehydrogenase A (LDHA) instead of mitochondrial oxidation<sup>30</sup>; hence, an elevated LDHA has been reported as an indicator of cancer prognosis. For example, in bladder cancer, LDHA expression is positively correlated with cancer proliferation and metastasis.<sup>31</sup> Likewise, our results showed that the upregulation of KHK, ALDOB, and LDHA in CCA cells is associated with tumorigenic phenomena. Lactate, which accumulation in cancer cells with high levels of glycolytic activity, can be eliminated into the extracellular compartment by monocarboxylate transporter 4 (MCT4), resulting in extracellular acidification in the tumor microenvironment, which favors tumor invasion and metastasis.<sup>3</sup> Likewise, the inhibition of MCT4 contributes to the reduction of tumor proliferation in colorectal cancer.<sup>32</sup> Overexpression of MCT4 has been recognized as a marker of glycolysis and lactate production, which is associated with cancers having a poor prognosis, such as breast, colorectal, and kidney cancers.<sup>32–35</sup> In addition, our data showed that GLUT5 affects the relative expression level of MCT4 in CCA cells. Similarly, the cancer inhibitory effect of a triterpenoid derivative from traditional Chinese medicine,  $\alpha$ -hederin, on lung cancer cell growth has been revealed to be mediated by the suppression of glycolysis and lactate production.<sup>36</sup> Remarkably, lactic acidosis in the tumor microenvironment, also from lactate export, can regulate EMT, involved in cancer progression.<sup>37,38</sup> Collectively, these findings support the hypothesis that upregulation of GLUT5 enhances glycolysis and ATP production in CCA cells, as the Warburg effect, via regulation of the fructose metabolic pathway, resulting in CCA progression (Fig. 6C).

Furthermore, in the tumor microenvironment, low oxygen level or hypoxia generally emerges as a promising feature of carcinogenesis, with HIF-1 $\alpha$  as a key regulator in cellular adaptation.<sup>39</sup> In tumor cells, HIF-1 $\alpha$  promotes survival by facilitating glucose uptake and modifying glucose metabolism; thus, HIF-1 $\alpha$  alters multiple glycolytic enzymes, such as hexokinase 2, phosphofructokinase 1, fructose-bisphosphate aldolase A, and pyruvate kinase.<sup>40</sup> In addition to glucose utilization, HIF-1 $\alpha$  has been reported as a regulator of lactate generation and elimination by controlling the expression of LDHA and MCT4.<sup>41,42</sup> During interaction between cancer cells and immune cells, lactate-MCT-HIF1 $\alpha$  has been identified to be correlated with metabolic reprogramming of macrophage polarization in gastric cancer.<sup>43</sup> Our results support the hypothesis that HIF-1 $\alpha$  plays a vital role in regulating energy metabolism in CCA through alterations in fructolysis (conversion of fructose to DHAP and GA) and glycolysis/Warburg effect. Notably, upregulation of HIF-1 $\alpha$  in response to hypoxia has an impact on the transcriptional activation of the gene encoding GLUT.<sup>44</sup> In trophoblast-derived cells, HIF-1 $\alpha$  promotes cellular glucose uptake via

knockdown cells in fructose-deficient and fructose-supplemented medium in (E) KKU-213A and (F) YSCC cells. \* Or # significant difference compared to siControl group in conditions of (+) Fructose or (-) Fructose treatment, respectively. One mark (\*, #) indicates  $P < 0.05$ , two marks indicate  $P < 0.01$ , three marks indicate  $P < 0.001$ .

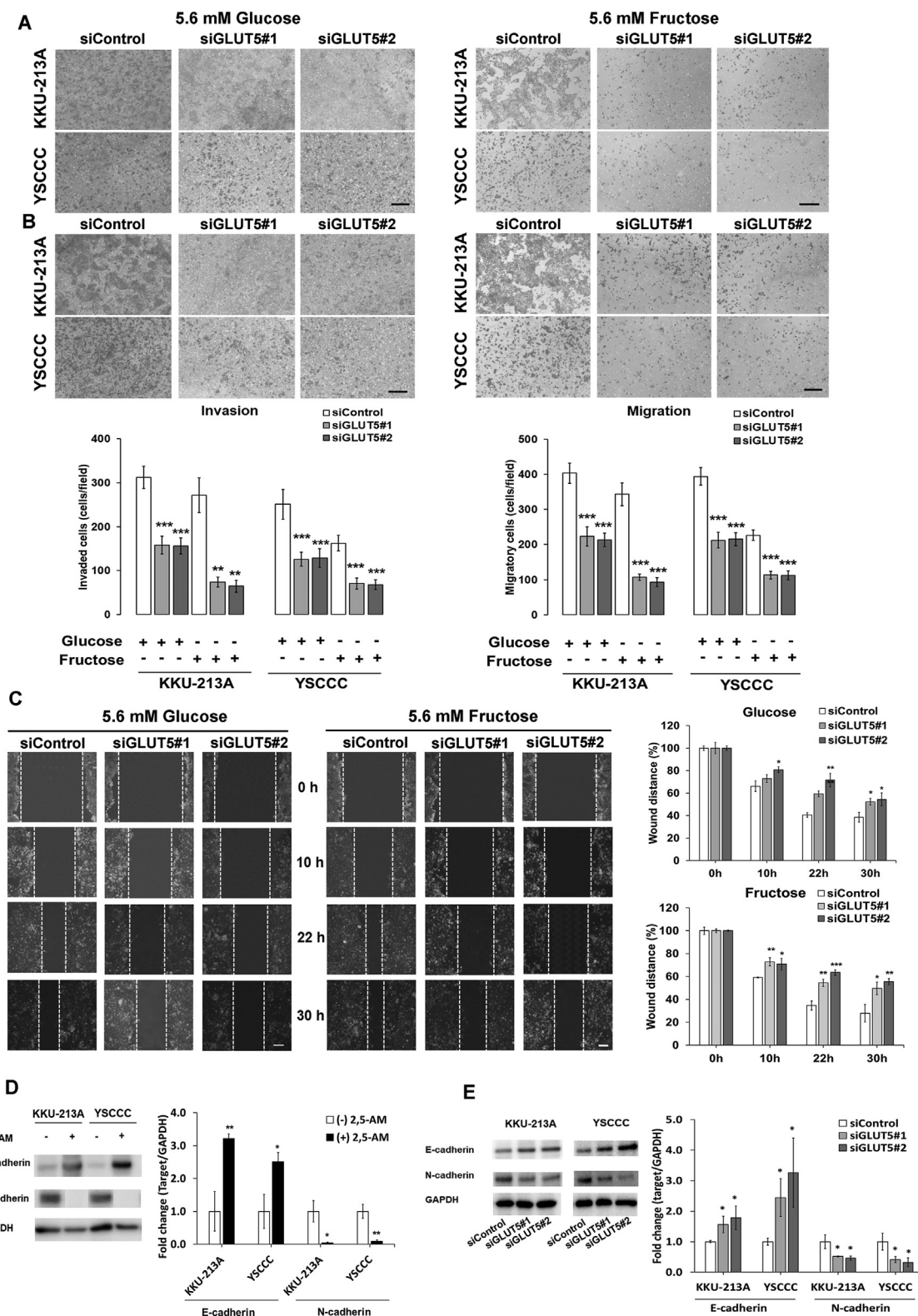


**Figure 4** Effect of GLUT5 downregulation on cell migration/invasion and EMT markers. Qualitative and quantitative analysis of (A) cell invasion and (B) cell migration of GLUT5 knockdown cells in differential sugar source. (C) Wound healing assay with relative distance of wound edges. Expression levels of EMT markers in GLUT5 knockdown cells using GLUT5 inhibitor (D) and gene knockdown by siRNA (E). \* Significant difference compared to the siControl group in each cell line. One mark (\*) indicates  $P < 0.05$ , two marks indicate  $P < 0.01$ , and three marks indicate  $P < 0.001$ .

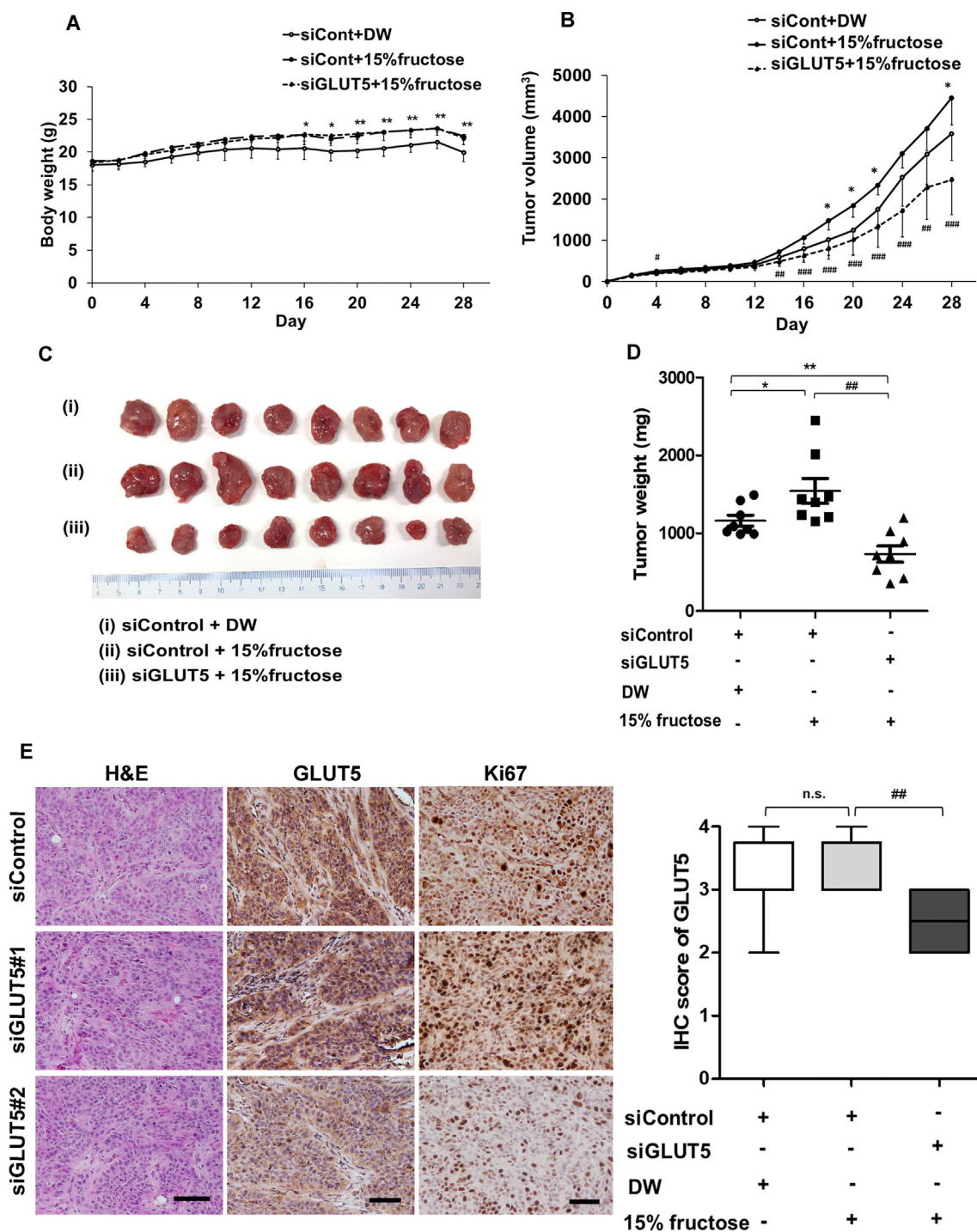


**Figure 5** *In vivo* study of tumor-inhibiting effect of GLUT5 knockdown CCA cells in nude mouse xenograft model. (A) Body weight, (B) tumor volume, (C) tumor from nude mouse xenografts, (D) tumor weight, and (E) H&E and IHC staining of GLUT5, and Ki67 in mouse tumor tissue. \* Significant difference compared to siControl + DW group. # Significant difference compared to siControl+15% fructose group. DW: distilled water. One mark (\*, #) indicates  $P < 0.05$ , two marks indicate  $P < 0.01$ , three marks indicate  $P < 0.001$ . n.s., not significant.

GLUT1 overexpression under hypoxic conditions,<sup>45</sup> as in ovarian and gastric cancers.<sup>46,47</sup> In neuronal cells, GLUT3 induction relies on HIF-1 $\alpha$  through the PI3K/Akt/mTOR dependent pathway.<sup>48</sup> Hamann et al reported that the transcription factor HIF-1 $\alpha$  regulates GLUT1 and GLUT5 in

breast cancer cells and tissues under hypoxic conditions.<sup>49</sup> Consistent with these findings, we further demonstrated the association between GLUT5-overproducing cells and HIF-1 $\alpha$  activation, indicating a close correlation of both genes in CCA progression (Fig. 6C).

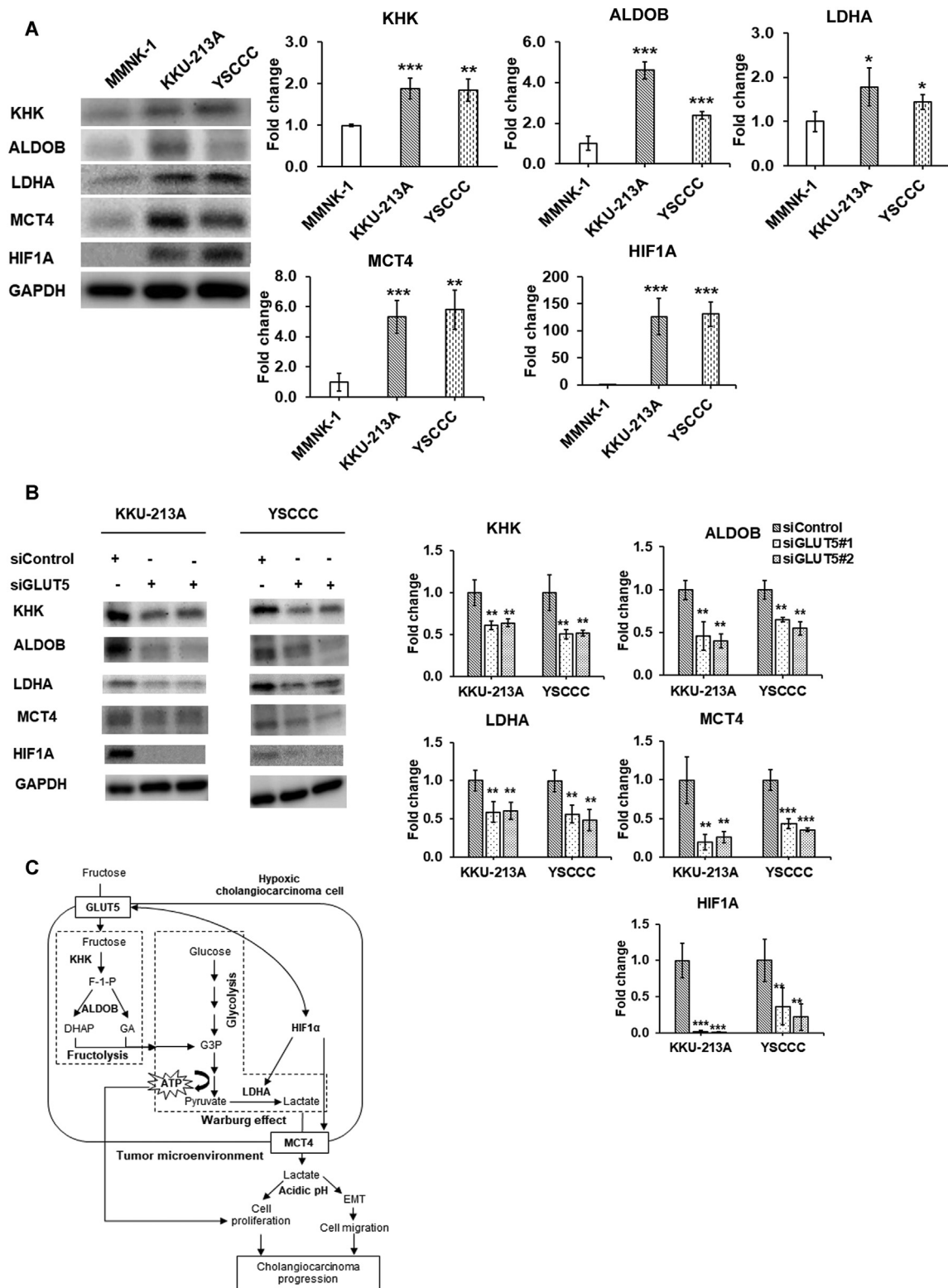


**Figure 6** Metabolic regulation of GLUT5 in CCA cells. **(A)** Expression levels of downstream molecules including KHK, ALDOB, LDHA, MCT4 and HIF1A between normal and CCA cells. \* Significant difference between normal and CCA cell lines. **(B)** Effects of GLUT5 knockdown on expression of downstream molecules. \* Significant difference compared to the siControl group in each cell line. One mark (\*) indicates  $P < 0.05$ , two marks indicate  $P < 0.01$ , and three marks indicate  $P < 0.001$ . **(C)** Possible mechanism of GLUT5-mediated tumorigenesis through the metabolic pathway in CCA cells. KHK, ketohexokinase; F-1-P, fructose-1-phosphate; ALDOB, aldolase B; DHAP, dihydroxyacetone phosphate; GA, glyceraldehyde; G3P, glyceraldehyde-3-phosphate; LDHA, lactate dehydrogenase; MCT4, monocarboxylate transporter; HIF1A, hypoxia-inducible factor 1 alpha.

In conclusion, the present study illustrated the principal role of GLUT5 in the tumorigenic phenomenon of human CCA by facilitating fructose uptake for cancer proliferation, enhancing tumor migration/invasion, and controlling EMT balance. Furthermore, our findings provide evidence that the overexpression of GLUT5 is implicated in the regulation of CCA metabolic pathway possessing downstream targets in the fructolysis-Warburg effect and hypoxia-inducible genes, which supports the emergence of GLUT5 as a novel therapeutic target in CCA.

## Ethics declaration

Human tissues from the Cholangiocarcinoma Research Institute of Srinagarind Hospital, Khon Kaen University, Thailand were approved by the Ethics Committee for Human Research (HE571283) of Khon Kaen University, Thailand. All patients provided written informed consent. The *in vivo* study was approved by the Committee of Animal Center of Mie University (approval no. 26-19-sai3).

## Author contributions

NS, KM and MM conceived and designed the study. NS performed the experiments, data analysis and prepared the manuscript. NM assisted preparation of mouse tissue for immunohistochemical staining. RT provided human CCA samples (KKU) and clinical data. NA contributed to RNA-seq data analysis. TK helped to perform the quality control assessment of RNA seq data. SK, SO, HK assisted in manuscript editing. All authors reviewed and approved the final version of manuscript.

## Conflict of interests

The authors declare that they have no conflict of interest.

## Funding

This work was supported by JSPS KAKENHI, Japan [No. JP16H05255, JP19H03884 (MM), JP17H04654 (NM)] and scholarship support from the Japanese Government (MEXT) provided to the author (NS).

## Availability of data and materials

Data sets used or analyzed during the current study can be obtained reasonably request of the corresponding author.

## Appendix A. Supplementary data

Supplementary data to this article can be found online at <https://doi.org/10.1016/j.gendis.2021.09.002>.

## References

- Hanahan D, Weinberg RA. Hallmarks of cancer: the next generation. *Cell*. 2011;144(5):646–674.
- Warburg O. On the origin of cancer cells. *Science*. 1956; 123(3191):309–314.
- de la Cruz-López KG, Castro-Muñoz LJ, Reyes-Hernández DO, García-Carrancá A, Manzo-Merino J. Lactate in the regulation of tumor microenvironment and therapeutic approaches. *Front Oncol*. 2019;9:1143.
- Jang M, Kim SS, Lee J. Cancer cell metabolism: implications for therapeutic targets. *Exp Mol Med*. 2013;45(10):e45.
- Krause N, Wegner A. Fructose metabolism in cancer. *Cells*. 2020;9(12):2635.
- Taskinen MR, Packard CJ, Borén J. Dietary fructose and the metabolic syndrome. *Nutrients*. 2019;11(9):1987.
- Charrez B, Qiao L, Hebbard L. The role of fructose in metabolism and cancer. *Horm Mol Biol Clin Investig*. 2015;22(2):79–89.
- Weng Y, Zhu J, Chen Z, Fu J, Zhang F. Fructose fuels lung adenocarcinoma through GLUT5. *Cell Death Dis*. 2018;9(5):557.
- Liu H, Huang D, McArthur DL, Boros LG, Nissen N, Heaney AP. Fructose induces transketolase flux to promote pancreatic cancer growth. *Cancer Res*. 2010;70(15):6368–6376.
- Zhao FQ, Keating AF. Functional properties and genomics of glucose transporters. *Curr Genomics*. 2007;8(2):113–128.
- Zwarts I, van Zutphen T, Kruit JK, et al. Identification of the fructose transporter GLUT5 (SLC2A5) as a novel target of nuclear receptor LXR. *Sci Rep*. 2019;9(1):9299.
- Fan X, Liu H, Liu M, Wang Y, Qiu L, Cui Y. Increased utilization of fructose has a positive effect on the development of breast cancer. *PeerJ*. 2017;5:e3804.
- Weng Y, Fan X, Bai Y, et al. SLC2A5 promotes lung adenocarcinoma cell growth and metastasis by enhancing fructose utilization. *Cell Death Discov*. 2018;4:38.
- Suwannakul N, Ma N, Midorikawa K, et al. CD44v9 induces stem cell-like phenotypes in human cholangiocarcinoma. *Front Cell Dev Biol*. 2020;8:417.
- Nakagawa T, Lanaspá MA, Millan IS, et al. Fructose contributes to the Warburg effect for cancer growth. *Cancer Metab*. 2020; 8:16.
- Samuel VT. Fructose induced lipogenesis: from sugar to fat to insulin resistance. *Trends Endocrinol Metabol*. 2011;22(2): 60–65.
- Strober JW, Brady MJ. Dietary fructose consumption and triple-negative breast cancer incidence. *Front Endocrinol*. 2019;10: 367.
- Ozawa T, Maehara N, Kai T, Arai S, Miyazaki T. Dietary fructose-induced hepatocellular carcinoma development manifested in mice lacking apoptosis inhibitor of macrophage (AIM). *Genes Cells*. 2016;21(12):1320–1332.
- Hussar P, Popovska-Percinac F, Blagoevska K, Järveots T, Dürütis I. Immunohistochemical study of glucose transporter GLUT-5 in duodenal epithelium in norm and in T-2 mycotoxicosis. *Foods*. 2020;9(7):849.
- Chen WL, Jin X, Wang M, et al. GLUT5-mediated fructose utilization drives lung cancer growth by stimulating fatty acid synthesis and AMPK/mTORC1 signaling. *JCI Insight*. 2020;5(3): e131596.
- Jin X, Liang Y, Liu D, et al. An essential role for GLUT5-mediated fructose utilization in exacerbating the malignancy of clear cell renal cell carcinoma. *Cell Biol Toxicol*. 2019;35(5): 471–483.
- Jin C, Gong X, Shang Y. GLUT5 increases fructose utilization in ovarian cancer. *Oncotargets Ther*. 2019;12:5425–5436.
- Chen WL, Wang YY, Zhao A, et al. Enhanced fructose utilization mediated by SLC2A5 is a unique metabolic feature of acute myeloid leukemia with therapeutic potential. *Cancer Cell*. 2016;30(5):779–791.
- Mellor KM, Bell JR, Wendt IR, Davidoff AJ, Ritchie RH, Delbridge LM. Fructose modulates cardiomyocyte excitation-

- contraction coupling and Ca<sup>2+</sup> handling in vitro. *PLoS One*. 2011;6(9):e25204.
25. Barone S, Fussell SL, Singh AK, et al. Slc2a5 (Glut 5) is essential for the absorption of fructose in the intestine and generation of fructose-induced hypertension. *J Biol Chem*. 2009;284(8):5056–5066.
  26. Włodarczyk J, Włodarczyk M, Zielińska M, Jędrzejczak B, Dziki Ł, Fichna J. Blockade of fructose transporter protein GLUT5 inhibits proliferation of colon cancer cells: proof of concept for a new class of anti-tumor therapeutics. *Pharmacol Rep*. 2021;73(3):939–945.
  27. Park GB, Jeong JY, Kim D. GLUT5 regulation by AKT1/3-miR-125b-5p downregulation induces migratory activity and drug resistance in TLR-modified colorectal cancer cells. *Carcinogenesis*. 2020;41(10):1329–1340.
  28. Merino B, Fernández-Díaz CM, Cózar-Castellano I, Perdomo G. Intestinal fructose and glucose metabolism in health and disease. *Nutrients*. 2019;12(1):94.
  29. Danhier P, Bański P, Payen VL, et al. Cancer metabolism in space and time: beyond the Warburg effect. *Biochim Biophys Acta Bioenerg*. 2017;1858(8):556–572.
  30. Cai Q, Lin T, Kamarajugadda S, Lu J. Regulation of glycolysis and the Warburg effect by estrogen-related receptors. *Oncogene*. 2013;32(16):2079–2086.
  31. Jiang F, Ma S, Xue Y, Hou J, Zhang Y. LDH-A promotes malignant progression via activation of epithelial-to-mesenchymal transition and conferring stemness in muscle-invasive bladder cancer. *Biochem Biophys Res Commun*. 2016;469(4):985–992.
  32. Kim HK, Lee I, Bang H, et al. MCT4 expression is a potential therapeutic target in colorectal cancer with peritoneal carcinomatosis. *Mol Cancer Ther*. 2018;17(4):838–848.
  33. Xiao S, Zhu H, Shi Y, Wu Z, Wu H, Xie M. Prognostic and predictive value of monocarboxylate transporter 4 in patients with breast cancer. *Oncol Lett*. 2020;20(3):2143–2152.
  34. Gotanda Y, Akagi Y, Kawahara A, et al. Expression of monocarboxylate transporter (MCT)-4 in colorectal cancer and its role: MCT4 contributes to the growth of colorectal cancer with vascular endothelial growth factor. *Anticancer Res*. 2013;33(7):2941–2947.
  35. Kim Y, Choi JW, Lee JH, Kim YS. Expression of lactate/H<sup>+</sup> symporters MCT1 and MCT4 and their chaperone CD147 predicts tumor progression in clear cell renal cell carcinoma: immunohistochemical and The Cancer Genome Atlas data analyses. *Hum Pathol*. 2015;46(1):104–112.
  36. Chang L, Fang S, Gu W. The molecular mechanism of metabolic remodeling in lung cancer. *J Cancer*. 2020;11(6):1403–1411.
  37. Cai H, Li J, Zhang Y, et al. LDHA promotes oral squamous cell carcinoma progression through facilitating glycolysis and epithelial–mesenchymal transition. *Front Oncol*. 2019;9:1446.
  38. Peppicelli S, Bianchini F, Calorini L. Extracellular acidity, a “reappreciated” trait of tumor environment driving malignancy: perspectives in diagnosis and therapy. *Cancer Metastasis Rev*. 2014;33(2–3):823–832.
  39. Jin X, Dai L, Ma Y, Wang J, Liu Z. Implications of HIF-1 $\alpha$  in the tumorigenesis and progression of pancreatic cancer. *Cancer Cell Int*. 2020;20:273.
  40. Moldogazieva NT, Mokhosoev IM, Terentiev AA. Metabolic heterogeneity of cancer cells: an interplay between HIF-1, GLUTs, and AMPK. *Cancers (Basel)*. 2020;12(4):862.
  41. Serganova I, Cohen IJ, Vemuri K, et al. LDH-A regulates the tumor microenvironment via HIF-signaling and modulates the immune response. *PLoS One*. 2018;13(9):e0203965.
  42. Ullah MS, Davies AJ, Halestrap AP. The plasma membrane lactate transporter MCT4, but not MCT1, is up-regulated by hypoxia through a HIF-1 alpha-dependent mechanism. *J Biol Chem*. 2006;281(14):9030–9037.
  43. Zhang L, Li S. Lactic acid promotes macrophage polarization through MCT-HIF1 $\alpha$  signaling in gastric cancer. *Exp Cell Res*. 2020;388(2):111846.
  44. Sadlecki P, Bodnar M, Grabiec M, et al. The role of Hypoxia-inducible factor-1  $\alpha$ , glucose transporter-1, (GLUT-1) and carbon anhydrase IX in endometrial cancer patients. *Biomed Res Int*. 2014;2014:616850.
  45. Hayashi M, Sakata M, Takeda T, et al. Induction of glucose transporter 1 expression through hypoxia-inducible factor 1 alpha under hypoxic conditions in trophoblast-derived cells. *J Endocrinol*. 2004;183(1):145–154.
  46. Yasuda M, Miyazawa M, Fujita M, et al. Expression of hypoxia inducible factor-1 alpha (HIF-1alpha) and glucose transporter-1 (GLUT-1) in ovarian adenocarcinomas: difference in hypoxic status depending on histological character. *Oncol Rep*. 2008;19(1):111–116.
  47. Hao LS, Liu Q, Tian C, et al. Correlation and expression analysis of hypoxia-inducible factor 1 $\alpha$ , glucose transporter 1 and lactate dehydrogenase 5 in human gastric cancer. *Oncol Lett*. 2019;18(2):1431–1441.
  48. Yu J, Li J, Zhang S, et al. IGF-1 induces hypoxia-inducible factor 1 $\alpha$ -mediated GLUT3 expression through PI3K/Akt/mTOR dependent pathways in PC12 cells. *Brain Res*. 2012;1430:18–24.
  49. Hamann I, Krysz D, Glubrecht D, et al. Expression and function of hexose transporters GLUT1, GLUT2, and GLUT5 in breast cancer-effects of hypoxia. *FASEB J*. 2018;32(9):5104–5118.